A Comparison of Several Techniques to Assign Heights to Cloud Tracers

STEVEN J. NIEMAN

Cooperative Institute for Meteorological Satellite Studies, Madison, Wisconsin

JOHANNES SCHMETZ

European Space Agency, European Space Operations Center, Darmstadt, Germany

W. PAUL MENZEL

NOAA/NESDIS, Madison, Wisconsin

(Manuscript received 27 July 1992, in final form 4 January 1993)

ABSTRACT

Satellite-derived cloud-motion vector (CMV) production has been troubled by inaccurate height assignment of cloud tracers, especially in thin semitransparent clouds. This paper presents the results of an intercomparison of current operational height assignment techniques. Currently, heights are assigned by one of three techniques when the appropriate spectral radiance measurements are available. The infrared window (IRW) technique compares measured brightness temperatures to forecast temperature profiles and thus infers opaque cloud levels. In semitransparent or small subpixel clouds, the carbon dioxide (CO_2) technique uses the ratio of radiances from different layers of the atmosphere to infer the correct cloud height. In the water vapor (H_2O) technique, radiances influenced by upper-tropospheric moisture and IRW radiances are measured for several pixels viewing different cloud amounts, and their linear relationship is used to extrapolate the correct cloud height. The results presented in this paper suggest that the H_2O technique is a viable alternative to the CO_2 technique for inferring the heights of semitransparent cloud elements. This is important since future National Environmental Satellite, Data, and Information Service (NESDIS) operations will have to rely on H_2O-derived cloud-height assignments in the wind field determinations with the next operational geostationary satellite. On a given day, the heights from the two approaches compare to within 60–110 hPa rms; drier atmospheric conditions tend to reduce the effectiveness of the H_2O technique. By inference one can conclude that the present height algorithms used operationally at NESDIS (with the CO_2 technique) and at the European Satellite Operations Center (ESOC) (with their version of the H_2O technique) are providing similar results. Sample wind fields produced with the ESOC and NESDIS algorithms using *Meteosat-4* data show good agreement.

1. Introduction

In the current operational use of four geostationary satellites [the United States Geostationary Operational Environmental Satellite (GOES), the European Meteorological Satellite (Meteosat), the Japanese Geostationary Meteorological Satellite (GMS), and the Indian Geostationary Satellite (Insat)], there continues to be considerable emphasis on inferring cloud motions apparent in a sequence of images. These cloud-motion vectors (CMV) provide information about atmospheric circulations and are especially valuable for weather forecast models in regions where other information is sparse, as over oceans. However, satellite-derived CMV production has been troubled by inaccurate height assignment of cloud tracers, especially in thin clouds that are semitransparent in the infrared window wavelengths. At the recent Workshop on Wind Extraction from Operational Meteorological Satellite Data (EUMETSAT 1991), there was a consensus that the present operational techniques for height assignment needed further review and that greater uniformity in these techniques and the associated global wind datasets is desirable for numerical weather prediction models.

Presently, heights of cloud-motion vectors are assigned using one of three techniques when the appropriate spectral radiance measurements are available. In opaque clouds, the infrared window (IRW) technique compares brightness temperatures to forecast temperature profiles and finds the level of best agreement, which is taken to be the level of the cloud. In semitransparent or small clouds, where the observed radiance contains contributions from below the cloud, this IRW technique often assigns the height to too low a level. Corrections for the semitransparency of the cloud are possible with the carbon dioxide slicing tech-

Corresponding author address: Dr. Paul Menzel, NOAA/NESDIS, University of Wisconsin, 1225 West Dayton Street, Madison, WI 53706.

nique (Menzel et al. 1983), where radiances from different layers of the atmosphere are used to infer the correct height. A similar concept is used in the water vapor intercept technique (Szejwach 1982), where radiances influenced by upper-tropospheric moisture and IRW radiances are measured for several pixels viewing different cloud amounts, and their linear relationship is used to extrapolate the correct cloud height. These three techniques are compared in this paper.

Each of the geostationary satellites in the international fleet measures radiances in different parts of the infrared spectrum. The portion of the spectrum dictates which cloud height assignment algorithm is possible. Insat measures radiances in the IRW (around 11 μm) and a window channel estimate of cloud height is used. Meteosat measures radiances in the IRW and H_2O (around 6.5 μm) absorption regions of the spectrum; thus, cloud height assignments are usually made using the H_2O–IRW intercept method. *GOES-7* measures radiances in the IRW, H_2O absorption, and CO_2 (around 13.5 μm) absorption regions of the spectrum, so height assignments can be made with both the H_2O–IRW intercept and the CO_2–IRW ratio methods. However, the *GOES-I* imager will measure IRW and H_2O but not CO_2 radiances, like Meteosat. The current *GMS-4* has neither H_2O nor CO_2 measuring capability, and height assignments must rely on the IRW technique, but *GMS-5* is adding an H_2O channel. Table 1 summarizes the spectral channels on the current and planned geostationary imaging instruments.

The purpose of this study is to verify that cloud heights of comparable quality can be produced by either the H_2O or the CO_2 approaches, since future National Environmental Satellite, Data, and Information Service (NESDIS), operational height assignments will have to come from the former. But there is further impetus for this work. The European Community (EC) shares one of its satellites with the United States, *Meteosat-3* (de Waard et al. 1992); understanding the relative performance of the NESDIS operational CO_2–IRW ratio heights and the European Satellite Operations Center (ESOC) operational H_2O–IRW intercept heights is necessary for the United States to begin production of CMVs with *Meteosat-3*. Finally, since the upcoming *GMS-5* will have a water vapor channel, comparable skill in assigning cloud heights is globally possible if viable H_2O–IRW height performance can be verified. As Table 1 indicates, the IRW and H_2O channels will be available on three of the four satellites used to produce operational cloud-motion vectors well into the next decade. (Insat plans are unknown at this time.)

TABLE 1. Spectral coverage on the current and planned geostationary satellites. Launch dates are indicated in parentheses. Five-year lifetimes are expected. The letter Y indicates this spectral channel is part of the instrument capability; N indicates it is not.

	Satellite (launch date)					
	GOES	GOES	Meteosat	Meteosat	GMS	GMS
	7 (87)	I (94)	3 (88)	SG1* (98)	4 (89)	5 (94)
		J (95)	4 (89)			
		K (99)	5 (91)			
		L (00)	6 (94)			
		M (04)	7 (96)			
			8 (?)			
Spectral coverage						
IRW	Y	Y	Y	Y	Y	Y
H_2O	Y	Y	Y	Y	N	Y
CO_2	Y	N	N	Y	N	N

* Indicates second generation

2. Algorithm description

a. The window channel estimate

A window channel (IRW) estimate of the cloud height is made by comparing infrared window (11.2 μm) brightness temperatures to numerical model forecast temperature profiles to infer the level of best agreement. For an opaque cloud this level is a good representation of the level of the cloud. However, movement of opaque clouds is not usually very representative of atmospheric flow.

Semitransparent clouds (such as cirrus) or subpixel clouds (small clouds not filling the sensor field of view) are often the best tracers for estimating cloud motion vectors, because they show radiance gradients that can readily be tracked and they are likely to be passive tracers of the flow at a single level. Unfortunately their height assignments are especially difficult. Since the fraction of the sensor field of view occupied by the cloud or the emissivity of the cloud is less than unity by an unknown amount, the brightness temperature T_b in the infrared window is usually an overestimate of the cloud temperature. Thus, heights for semitransparent or subpixel clouds inferred directly from the observed T_b and an available temperature profile are consistently low.

In the operational production of wind fields at NESDIS, the window channel estimate averages the infrared window brightness temperatures T_b of the coldest 25% of pixels in the tracer selection area of about 100 km on a side (Merrill 1989). A 6-h forecast model is the source of the temperature profile. The window channel estimate is used for low clouds (below 600 hPa) and when other techniques experience problems.

b. The CO_2–IRW ratio algorithm

The CO_2–IRW ratio technique calculates the spectral radiative transfer in an atmosphere with a single high cloud layer; it accounts for any semitransparency of the cloud. For a given cloud element in a field of view (FOV) the radiance observed $R(N)$ in spectral band N can be written

$$R(N) = (1 - nE)R_{c1}(N) + nER_{bcd}(N, P_c), \quad (1)$$

where $R_{c1}(N)$ is the corresponding clear-sky radiance, $R_{bcd}(N, P_c)$ is the corresponding radiance if the FOV were completely covered with an opaque or "black" cloud at pressure level P_c, n is the fraction of the FOV covered with cloud, and E is the cloud emissivity. In Eq. (1) for a given radiance observation, when the emissivity is overestimated, the cloud-top pressure is also overestimated (putting the cloud too low in the atmosphere).

Opaque cloud radiance can be calculated from

$$R_{bcd}(N, P_c) = R_{c1}(N) - \int_{P_c}^{P_s} t(N, p) \frac{dB[N, T(p)]}{dp} dp, \quad (2)$$

where P_s the surface pressure, P_c the cloud pressure, $t(N, p)$ the fractional transmittance of radiation of spectral band N emitted from the atmospheric pressure level p arriving at the top of the atmosphere ($p = 0$), and $B[N, T(p)]$ the Planck radiance of spectral band N for temperature $T(p)$. The second term on the right represents the decrease in radiation from clear conditions introduced by the opaque cloud.

Determination of cloud-top pressure proceeds as follows. The difference in clear and cloudy radiances is measured with VAS [VISSR (Visible–Infrared Spin Scan Radiometer) Atmospheric Sounder] for the infrared window (11.2 μm, VAS band 8) and the CO_2 channels (13.3 μm, VAS band 5). It is also calculated in a radiative transfer formulation. Equating the measured and calculated ratios of IRW and CO_2 channel radiance differences yields

$$\frac{R(CO_2) - R_{c1}(CO_2)}{R(IRW) - R_{c1}(IRW)} = \frac{nE(CO_2)[R_{bcd}(CO_2, P_c) - R_{c1}(CO_2)]}{nE(IRW)[R_{bcd}(IRW, P_c) - R_{c1}(IRW)]}. \quad (3)$$

Since the emissivities of ice clouds and the cloud fractions for the IRW and CO_2 channels are roughly the same, the cloud-top pressure of the cloud within the FOV can be specified. The left-hand side of the equation is evaluated using measured radiances for IRW and CO_2 channels and clear radiances for the same two channels, which are inferred from the first-guess sounding and analyzed surface temperatures interpolated to the target point. The right-hand side is computed for a series of possible cloud pressures, and the cloud tracer is assigned the pressure that best satisfies the equation.

The 11.2- and 13.3-μm channels have been suggested in the work of Eyre and Menzel (1989) because the 13.3-μm channel is sensitive to radiation emitted from most tropospheric features, yet the transmittance through the atmosphere is different enough from the 11-μm channel to produce a noticeable contrast. Additionally, the emissivity of thin cirrus clouds in these two spectral bands is very similar (Ackerman and Smith 1989).

The observed radiances used in the above calculation are obtained using a "cold sampling" procedure. Data are taken from an area roughly 100 km on a side, centered on the target point, and a histogram of the infrared window brightness temperatures is calculated. Radiances for both channels are averaged for the coldest 25% of the pixels in the window channel. The histogram is also used to modify the surface (skin) temperature that appears in the computation of the clear column radiance; the warmer of the 90th-percentile T_b and the analyzed surface temperature (using model forecast and surface reports) are used in the forward calculation.

The CO_2–IRW ratio fails when the difference between the observed and clear radiances in either channel is less than the instrument noise (0.2 mW m^{-2} sr^{-1} cm for 11.2 μm and 1.5 mW $m^{-2}sr^{-1}$ cm for 13.3 μm). This happens for low broken cloud or very thin cirrus. Another difficulty occurs in two-cloud-layer situations; the CO_2–IRW ratio yields a height somewhere between the two cloud layers (Menzel et al. 1992). Tracer selection for CMVs attempts to avoid multiple cloud layers. The CO_2–IRW ratio also experiences problems with very high opaque clouds, where the clear–cloudy differences between the channels are nearly identical and the ratio is almost invariant with pressure above a certain altitude. In this situation the window channel estimate is adequate.

In the study of Wylie and Menzel (1989), the CO_2 slicing cloud heights derived from VAS data (four channels including 11.2, 13.3, 14.0, and 14.2 μm) were compared to three other independent sources of cloud height information. Thin clouds above 600 hPa were the focus of this work. For about 30 different opaque clouds ranging from 850 to 300 hPa, the CO_2 heights were within 40 hPa rms of cloud heights inferred from radiosonde moisture profiles. In 100 comparisons with lidar scans of cirrus clouds above 600 hPa, the CO_2 heights were 70 hPa lower on average and were within 80 hPa rms. Satellite stereo parallax measurements in 100 cirrus clouds above 400 hPa compared to within 40 hPa rms. The CO_2 pressures for all of these clouds were within 50 hPa of the other cloud-top pressure estimate. This uncertainty in pressure converts to different height uncertainties at different atmospheric levels; for example, 50 hPa represents an uncertainty of about 1.5 km at 200 hPa and about 0.6 km at 600 hPa (for a midlatitude winter atmosphere). In the study of Eyre and Menzel (1989), the CO_2–IRW ratio (two-channel) approach was found to be comparable with the CO_2 slicing (four-channel) approach; for high clouds there was no discernible difference and for mid-level clouds the two approaches were within 40 hPa for thin to thick clouds.

c. The H_2O–IRW intercept method

The H_2O–IRW intercept height assignment is predicated on the fact that radiances in one spectral band observing a single cloud layer will vary linearly with the radiances in another spectral band as a function of cloud amount in the FOV. Thus, a plot of H_2O (6.7 μm) radiances versus IRW (11.2 μm) radiances in a scene of varying cloud amount will be nearly linear. These radiance measurements are used in conjunction with radiative transfer calculations for both spectral channels; Eq. (2) is used to calculate the radiance at the top of the atmosphere emanating from opaque clouds at different levels in an atmosphere whose temperature and humidity are specified by a numerical weather prediction model. The intersection of measured and calculated radiances will occur at clear-sky (cloud amount of zero) and opaque cloud radiances (cloud amount of one). The cloud-top temperature (and, hence, the pressure) is extracted from the cloud radiance intersection. Figure 1 shows an example of this process. The linear fit to the measured radiances is shown to intersect with the curve of calculated radiances when the radiance is emanating from the surface (clear sky) and from an opaque cloud at the correct pressure.

The linear relationship of the radiances in the IRW and H_2O channels can be seen in Eq. (3) by substituting H_2O for CO_2. The radiance change in H_2O over the radiance change in IRW is independent of cloud fraction N, thus indicating constant slope for single-level clouds. Thus, all radiance measurement pairs, $R(H_2O)$ and $R(\text{IRW})$, viewing different amounts of a single-layer cloud at pressure P_c, lie on a straight line.

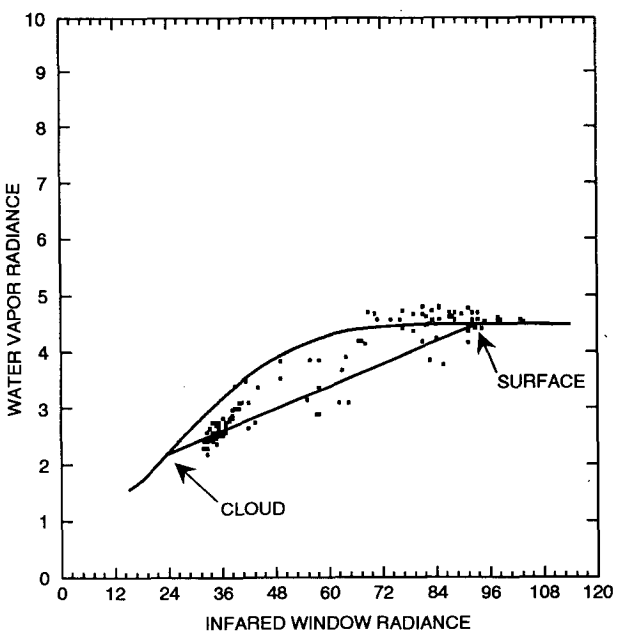

FIG. 1. Measured radiances (mW m^{-2} sr^{-1} cm) for fields of view partially filled with clouds. The curve represents the forward calculations of radiance for both spectral channels for opaque clouds at different levels in the atmosphere. The straight line connects the centers of the warmest and coldest clusters of measured radiances and is extrapolated to intersect the curve and thus identify the height of the cloud.

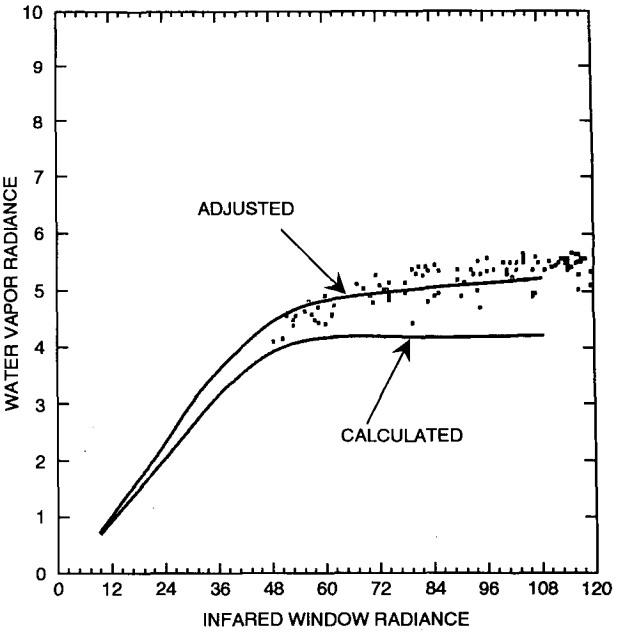

FIG. 2. Example showing the adjustment applied to the forward calculations of the H_2O radiance (mW m^{-2} sr^{-1} cm) when calculated and measured values disagree. The calculated H_2O radiances (lower curve) have been adjusted (upper curve) to agree with the average measured H_2O radiance of the warmest cluster.

The H_2O–IRW intercept method requires clear- and cloudy-sky radiance measurements in both the IRW and H_2O spectral channels. Further, combined use of calculated and measured radiances demands an accurate calibration.

The measured radiances used to infer the linear relationship between H_2O and IRW radiances are the average radiances for the cluster of clearest (warmest) fields of view and the cluster of the cloudiest (coldest) fields of view within the observational area. Radiances from an area roughly 100 km on a side, centered on the target point, are plotted and grouped into several clusters with differing cloud amounts. When the calculated H_2O radiances for clear sky are less than the measured H_2O radiances, the calculated H_2O radiances are adjusted to agree with the measured clear-sky H_2O radiances; the difference is attributed to an inaccurate guess profile (especially over the oceans) that is used in the computation of the clear column radiance (see Fig. 2). Calculated warm radiances that are greater than the measured radiances are not adjusted since the low measurement may be the result of cloud contamination. Note that the H_2O–IRW intercept method use of the cluster approach to designate clearest and cloudiest radiances is intrinsically different from the CO_2–IRW

ratio technique selection of the coldest 25% as cloud and the warmest 10% or the surface analysis as clear.

The cluster analysis algorithm used here is a modified version of the bivariate asymmetric Gaussian histogram analysis (Rossow et al. 1985; Tomassini 1981). Sufficiently homogeneous cloud and surface features within the observational area are revealed as clusters when the corresponding IRW and H_2O radiances are plotted against each other. Gaussian distribution functions are fitted separately to either side of the peaks in the IRW and H_2O radiance histograms.

The identification of each cluster involves ten steps. (i) A one-dimensional histogram with increments of one radiance unit (1 mW m^{-2} sr^{-1} cm) is constructed using available IRW radiance data from pixels not previously assigned to a cluster. (ii) A five-point smoothing is applied to the IRW histogram. (iii) The maximum frequency of the IRW histogram is identified. (iv) Separate Gaussian curves are fitted to each side of the peak; the variance of each curve is chosen to be the average variance obtained when a two-point method is applied to the frequency at the peak paired with the frequency 1, then 2, and then 3 radiance units from the peak. (v) All points within three standard deviations of the peak are then selected for further processing. (vi) A one-dimensional histogram is constructed from H_2O radiance data corresponding to those pixels chosen in the IRW selection process described in step (v). (vii) A three-point smoothing is applied to the H_2O histogram; a smaller smoothing is applied to H_2O (three point) than to IRW (five point) since the range of radiance values in the H_2O is only about 20 radiance units compared to the IRW range of about 100 radiance units. (viii) The maximum frequency in the H_2O histogram is identified. (ix) Separate Gaussian curves are chosen, as in (iv), to describe the relationship on each side of the peak. And finally, (x) all points within three standard deviations of the peak are then chosen to comprise the cluster.

The clustering procedure begins with all available pixels in the observational area (roughly 100 km on a side) and continues until seven clusters have been defined or until the histograms have become too flat for the method to continue. All pixels within the target area need not be assigned to a cluster; extreme values are excluded. All pixels falling within three standard deviations of a histogram peak meet selection criteria. The clearest (warmest) cluster and the cloudiest (coldest) cluster are used to infer the linear relationship between the H_2O and the IRW radiances as a function of cloud amount.

Since the H_2O radiances are primarily emanating from the upper troposphere, height determinations below 600 hPa are screened out.

TABLE 2. IRW, CO_2–IRW, and H_2O–IRW height assignments for cloud tracers using VAS radiances from 20° to 50°N and 50° to 100°W for 29–31 January 1992.

	Mean cloud-top pressure (hPa)	Scatter wrt mean (hPa)	rms deviation (hPa) wrt CO_2–IRW	rms deviation (hPa) wrt H_2O–IRW
29 Jan 1992 (87 tracers)				
IRW	390	101	123	133
CO_2–IRW	314	59	—	66
H_2O–IRW	304	60	66	—
30 Jan 1992 (51 tracers)				
IRW	434	93	82	137
CO_2–IRW	378	81	—	82
H_2O–IRW	324	51	82	—
31 Jan 1992 (61 tracers)				
IRW	438	103	107	156
CO_2–IRW	360	107	—	107
H_2O–IRW	319	78	107	—
All three days (199 tracers)				
IRW	416	102	109	141
CO_2–IRW	344	87	—	85
H_2O–IRW	314	65	85	—

3. Intercomparison results

Many of the intercomparisons were performed in the overlap region of the VAS and *Meteosat-3;* this occurs in the Atlantic Ocean. The results presented are mostly for single-cloud-layer tracers from the North Atlantic region from 20° to 50°N and from 50° to 100°W. As ground and aircraft observations of cloud height are sparse in this region, the CO_2–IRW ratio pressure estimates were used as a reference. The accuracy of the CO_2 estimates is well documented (Wylie and Menzel 1989; Menzel et al. 1992). While the comparisons reported here do not yield a measure of absolute accuracy, they do provide insight into the relative performance of the various height estimation algorithms.

a. Comparison of VAS CO_2–IRW and H_2O–IRW heights

Initial comparison of these three height assignment techniques was accomplished with data from VAS in January 1992. The multispectral imaging from VAS measures IRW (10.4–12.1 μm) radiances from 8-km FOVs and H_2O (6.4–7.1 μm) and CO_2 (13.2–13.5 μm) radiances from 16-km FOVs. Cloud elements were selected by the autowindco procedure (Merrill et al. 1991), which divides the entire image into cells (roughly 100 km on a side) and selects targets based on the overall brightness and contrast of the scene. Height assignments were made with all three methods described in the previous section. Table 2 presents the

results corresponding to 200 targets in midlatitudes (20°–50°N, 50°–100°W) for 29, 30, and 31 January 1992. Mean cloud-top pressures for all the height assignments using a single technique are calculated, and the rms scatter about that mean is also calculated; the scatter is due to natural variability in the cloud heights for these days as well as technique inaccuracy. The rms deviation of heights for all the tracers using one technique with respect to those using another technique are also presented; this value represents the deviation of one technique with respect to another.

The H_2O height assignment is on average 30 hPa higher in the atmosphere than the CO_2 height assignment. The IRW heights, without benefit of any semitransparency correction are about 70 hPa lower in the atmosphere than the CO_2 height assignment on average. Figure 3 shows the scatterplots for these three days. The H_2O–IRW and CO_2–IRW cloud-top pressures in Fig. 3a fall close to the line of one-to-one correspondence; agreement is within 50 hPa rms for the top of the troposphere and drops off to 100 hPa rms near 600 hPa. Both techniques show more skill higher in the troposphere. The IRW cloud-top pressures in Figs. 3b and 3c are noticeably below the line of one-to-one correspondence. Some of the IRW cloud-top pressures are unrealistically low in the atmosphere, due to the semitransparency of the high-cloud tracers selected. IRW versus H_2O–IRW and CO_2–IRW estimates show larger disagreement near the top of the troposphere (about 150 hPa rms) than at 600 hPa (about 100 hPa rms).

On 29 January the H_2O–IRW intercept and the CO_2–IRW ratio yield similar mean cloud-top pressures (304 and 314 hPa, respectively), and the scatter (60 and 59 hPa, respectively) in the heights of the clouds observed with respect to the average height is almost the same. The statistical properties for both methods are the same. The rms deviation between the two methods is 66 hPa, indicating very good agreement. The IRW heights were much lower on average (390 hPa) and showed more scatter (101 hPa); the absence of any semitransparency correction is the probable cause.

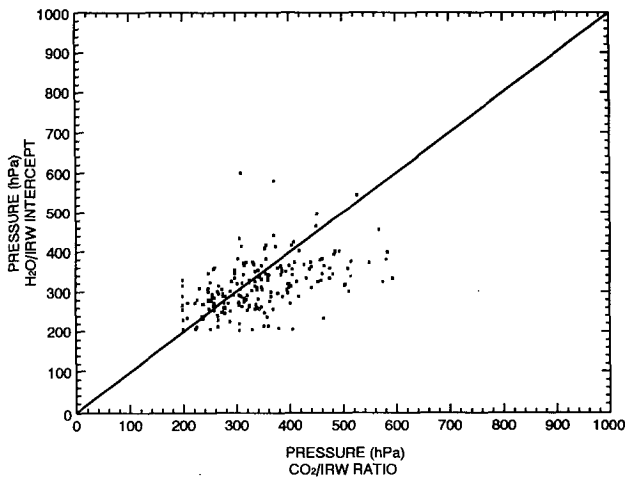

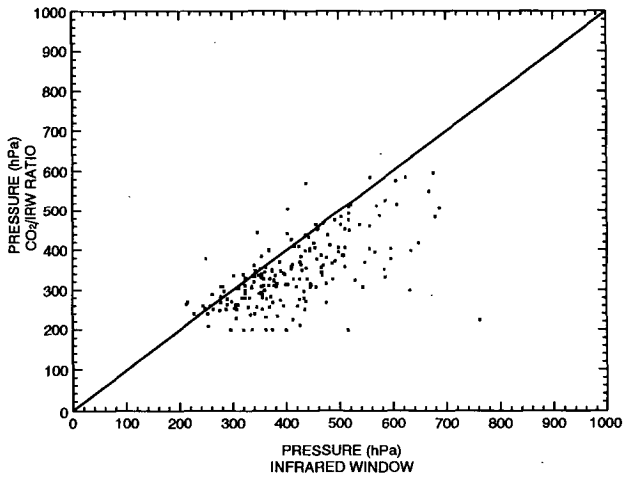

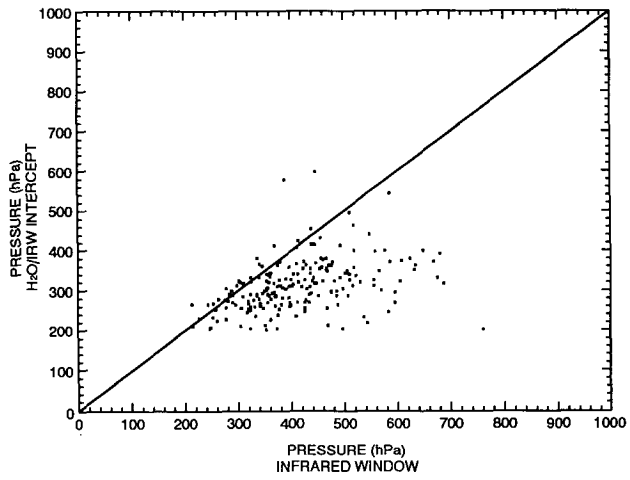

FIG. 3. (a) Scatterplot of cloud-top pressures (hPa) corresponding to all three days of the data presented in Table 2 for CO_2 slicing technique vs H_2O intercept technique. (b) Scatterplot of cloud-top pressures (hPa) corresponding to all three days of the data presented in Table 2 for CO_2 slicing technique vs IR window technique. (c) Scatterplot of cloud-top pressures (hPa) corresponding to all three days of the data presented in Table 2 for H_2O intercept technique vs IR window technique.

On 30 January, the H_2O–IRW intercept produced cloud-top pressures 54 hPa higher in the atmosphere than the CO_2–IRW ratio. The scatter of the H_2O–IRW results is only 51 hPa as opposed to 81 hPa in the CO_2–IRW results. The rms deviation between the methods is 82 hPa. Explanation of these somewhat degraded results one day later may rest in the fact that the upper troposphere was drier on 30 January than on the previous day; this is noticeable by the increase in mean water vapor channel brightness temperature over the cloud tracers from 232 K on 29 January to 235 K on 30 January. In a drier atmosphere, clouds will exhibit lower emissivity in the infrared window, and thus, the IRW channel measures warmer radiances; however, the water vapor attenuation in the H_2O channel remains disproportionately high. (The H_2O channel is sensitive to only the first few tenths of a millimeter of water vapor.) This combination of less-sensitive IRW and more-sensitive H_2O will produce large slopes between cloudy- and clear-sky clusters and yield H_2O–IRW intercept estimates that are too high in the atmosphere (Schmetz et al. 1993). The IRW technique again places the clouds much lower than either of the other two techniques and scatters them more.

On 31 January, the H_2O–IRW intercept produced cloud-top pressures 41 hPa higher in the atmosphere than the CO_2–IRW ratio. The scatter of the H_2O–IRW results is only 78 hPa as opposed to the 107 hPa of the CO_2–IRW results. Root-mean-square deviation between the methods is 107 hPa. Drier conditions again prevailed (the mean water vapor channel brightness temperature over the cloud tracers has now risen to 237 K on 31 January), and it is suspected that the H_2O–IRW intercept is suppressing some of the actual variation in the cloud-top pressures.

b. *Comparison of VAS H_2O–IRW and Meteosat-3 H_2O–IRW heights*

Height assignments using the same technique but different sensors were compared next. VAS H_2O–IRW intercept estimates of cloud-top pressure were compared to *Meteosat-3* H_2O–IRW intercept estimates for the same three days, 29–31 January 1992. *Meteosat-3* measures IRW (10.7–12.4 μm) radiances and H_2O (5.8–7.3 μm) radiances from 5-km FOVs. As with VAS, the *Meteosat-3* cloud tracer elements were selected by the autowindco procedure. Table 3 presents the comparison of the cloud-top pressures for close to 100 cloud elements collocated in *Meteosat-3* and *GOES-7* VAS 1130 UTC images from these three days; collocation was within 50 km. The mean cloud-top pressures agree to within 9 hPa and both show rms scatter about the mean of about 80–90 hPa; rms deviation between the two datasets is 94 hPa. Some of the differences in the cloud heights may be attributed to the different sized FOVs and the different spectral response functions. Figure 4 shows the scatterplots of the VAS and Meteosat H_2O–IRW intercept cloud-top pressure estimates; a few gross disagreements are evident. Overall the agreement is very good, indicating that Meteosat and GOES produce similar results using the H_2O–IRW intercept method.

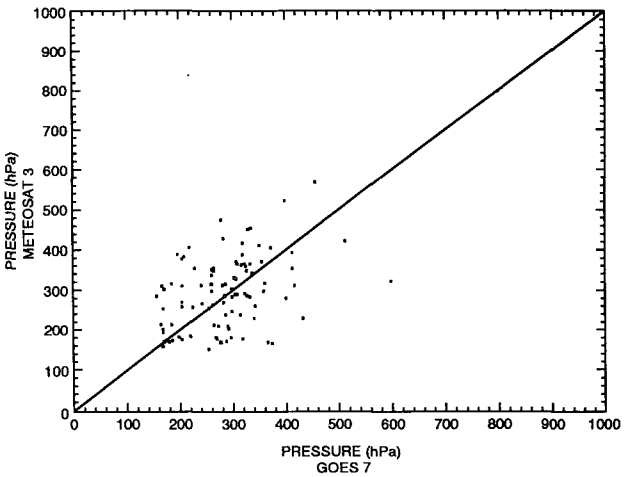

FIG. 4. Scatterplots of collocated VAS (*GOES-7*) and *Meteosat-3* H_2O intercept technique cloud-top pressure estimates for cloud tracers on 29–31 January 1992.

c. *Comparison of CIMSS H_2O–IRW and operational ESOC heights with Meteosat-4*

Finally, height assignment from CIMSS (Cooperative Institute for Meteorological Satellite Studies) and ESOC using the same sensor were compared in an attempt to verify that future NESDIS operational height assignments with *Meteosat-3* or *GOES-I* will have comparable quality to those generated operationally

TABLE 3. Collocated *Meteosat-3* (M-3) and *GOES-7* (G-7) H_2O height assignments for cloud tracers on 29–31 January 1992.

All three days (97 tracers)	Mean cloud-top pressure (hPa)	Scatter wrt mean (hPa)	rms deviation (hPa) wrt G-7 H_2O
G-7 H_2O	285	80	—
M-3 H_2O	294	89	94

TABLE 4. Collocated CIMSS and ESOC *Meteosat-4* (M-4) H_2O height assignments for upper-level (150–600 hPa) cloud tracers on 21 March, 27 April, and 30 April 1992.

Both days (136 tracers)	Mean cloud-top pressure (hPa)	Scatter wrt mean (hPa)	rms deviation (hPa) wrt *CIMSS* M-4 H_2O
CIMSS M-4 H_2O	272	97	—
ESOC M-4 H_2O	297	100	77

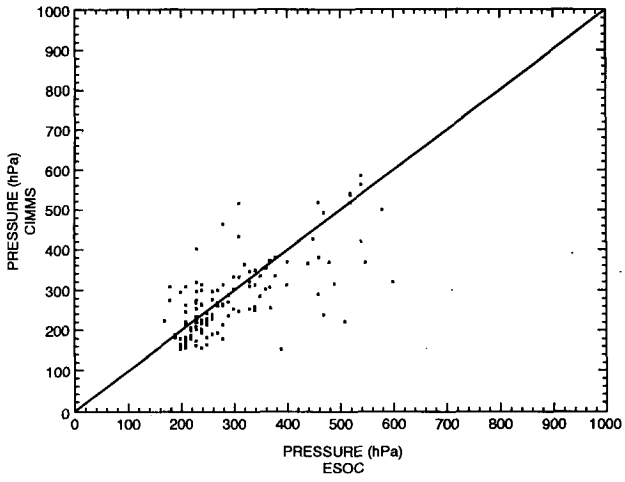

FIG. 5. Scatterplots of collocated CIMSS and ESOC *Meteosat-4* cloud-top pressure estimates for upper-level (150–600 hPa) cloud tracers on 21 March, 27 April, and 30 April 1992.

by ESOC. The H_2O–IRW intercept algorithm was applied to the *Meteosat-4* data, and the cloud-height results were compared to the heights of the operational ESOC cloud-motion winds (Schmetz et al. 1993). ESOC also estimates cloud heights with an H_2O–IRW intercept approach. Table 4 shows the comparison of CIMSS and ESOC height assignments for upper-level (between 150 and 600 hPa) cloud tracers collocated to within 50 km for 21 March, 27 April, and 30 April 1992; it is in the upper levels that the semitransparency correction of the H_2O–IRW intercept method is most important. The ESOC and CIMSS mean cloud-top pressures agree to within 25 hPa and both show scatter of about 100 hPa; rms error between the two height datasets is about 77 hPa. Figure 5 shows the relatively good agreement of the two algorithms; while some disagreements of more than 200 hPa are evident, most disagreements are less than 75 hPa. To put this agreement in perspective, recall that the skill of the CO_2 technique has been shown to be about 50 hPa (Wylie and Menzel 1989).

4. Example wind fields

While the thrust of this paper is the intercomparison of several techniques for assigning cloud tracer heights, the utility of height assignments is usually evaluated in the quality of the wind fields they help produce. Therefore this section presents wind fields produced in the United States and compares them to those produced in Europe. The previous section demonstrated that the height assignments are similar; the sample wind fields show that international commonality of wind production is at hand. The cloud-motion vectors for the Northern Hemisphere from *Meteosat-4* infrared window channel imagery determined with the CIMSS wind algorithm are compared to the operational ESOC winds.

The CIMSS winds (see Fig. 6 for a sample wind field) were produced using the automated winds algorithm for mid- and upper-level winds (Merrill et al. 1991). This technique uses an objective pattern matching technique (Space Science and Engineering Center 1985) in a sequence of images to estimate a velocity. Cloud heights are assigned to the higher of the H_2O–IRW intercept and the IRW estimates. The CIMSS procedure has been transferred to NESDIS for operational use with a few differences. Wind produc-

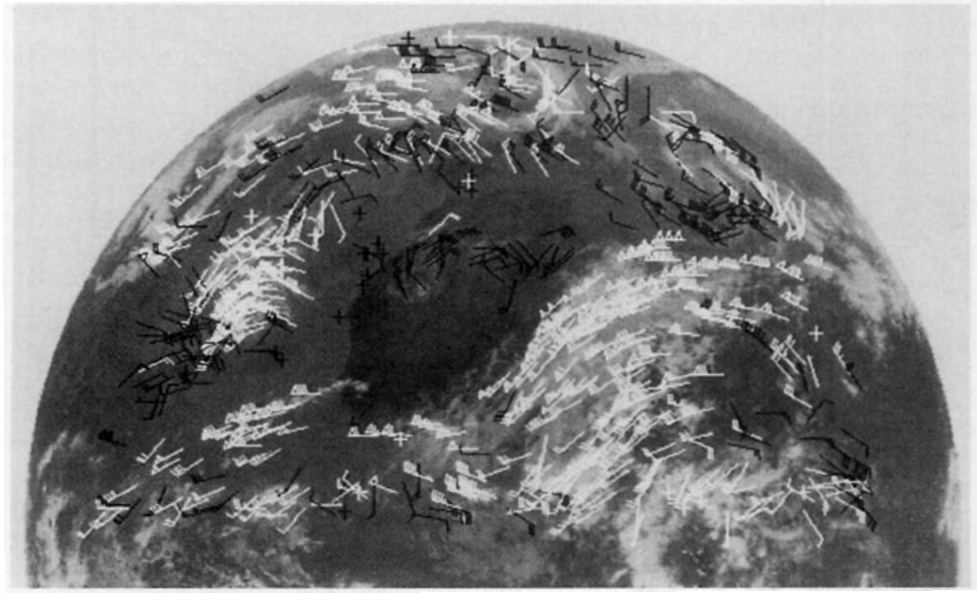

FIG. 6. Cloud-motion vectors produced from *Meteosat-4* IR imagery using the CIMSS wind system for 1600 UTC 21 March 1992. Upper-level (100–400 hPa) vectors are indicated in white, lower-level (400–950 hPa) vectors in black.

tion within NESDIS operations includes some additional steps. The preliminary height assignments are modified objectively as necessary after assimilation with other wind estimates (Hayden and Velden 1991); however, in this sample wind field such a height adjustment was not performed so that unmodified H_2O–IRW intercept heights could be inspected. Following objective quality control, manual quality control is performed at an interactive computer terminal modeled after the Man–computer Interactive Data Access System (Suomi et al. 1983); wind fields are investigated for excessive acceleration in successive image pairs, horizontal and vertical consistency of neighboring vectors, and excessive deviations from the first guess and rawinsondes. Manual quality control was not performed on the CIMSS wind fields presented here.

The ESOC winds (see Fig. 7 for a sample wind field) were produced with the operational algorithms described in Schmetz et al. (1993). These also use automatic tracking based on cross correlation of radiance features. A notable addition to the ESOC processing is that the upper-level cloud features are enhanced by image filtering before the cloud tracking commences. The heights of semitransparent and broken subpixel clouds are also estimated with an H_2O–IRW approach. Figures 6 and 7 indicate that similar coverage and vector density was accomplished by both the CIMSS and ESOC techniques.

Data from 21 March, 27 April, and 30 April 1992 produced 136 collocated tracers; the CIMSS winds are valid for 1600 UTC while the ESOC operational winds are valid for 1700 UTC. Spatial collocation is within a circle of 0.5° latitude and longitude. The hour time difference was unavoidable due to limitations in the CIMSS access to *Meteosat-4* data. For all three days, on average, the CIMSS winds are 0.4 m s^{-1} slower and the vector rms difference (without any bias adjustment) is 4.2 m s^{-1}. The rms difference in direction is 10.3° and the rms difference in speed is 3.2 m s^{-1}. Figure 8 shows the collocated cloud-motion vectors (CMV) from the CIMSS and ESOC systems for 21 March 1992; overall agreement is apparent although some differences in vector magnitude and direction are noticeable.

It can be expected that operational wind production from GOES and Meteosat will generate compatible results. The quarterly statistics monitoring operational wind fields against radiosonde and aircraft reports generated by the European Centre for Medium-Range Weather Forecasts for 1992 support this assertion (ECMWF 1992).

5. Conclusions

The results presented in this paper suggest that the H_2O–IRW intercept technique is a viable alternative to the CO_2 slicing technique for inferring the heights of semitransparent cloud elements. On a given day the heights from the two approaches compare to within 60–110 hPa rms; drier atmospheric conditions tend to reduce the effectiveness of the H_2O–IRW intercept technique. The results compare well with the validation of the CO_2 heights versus lidar and stereo cloud heights (Wylie and Menzel 1989). The theoretical study of Eyre and Menzel (1989) suggests that in general the CO_2 heights will be more representative than the H_2O–IRW heights; this is confirmed by the degraded performance of the H_2O–IRW heights in drier atmospheres. The infrared window channel technique consistently places the semitransparent cloud elements too low in the atmosphere by 100 hPa or more; only in more opaque clouds does it perform adequately.

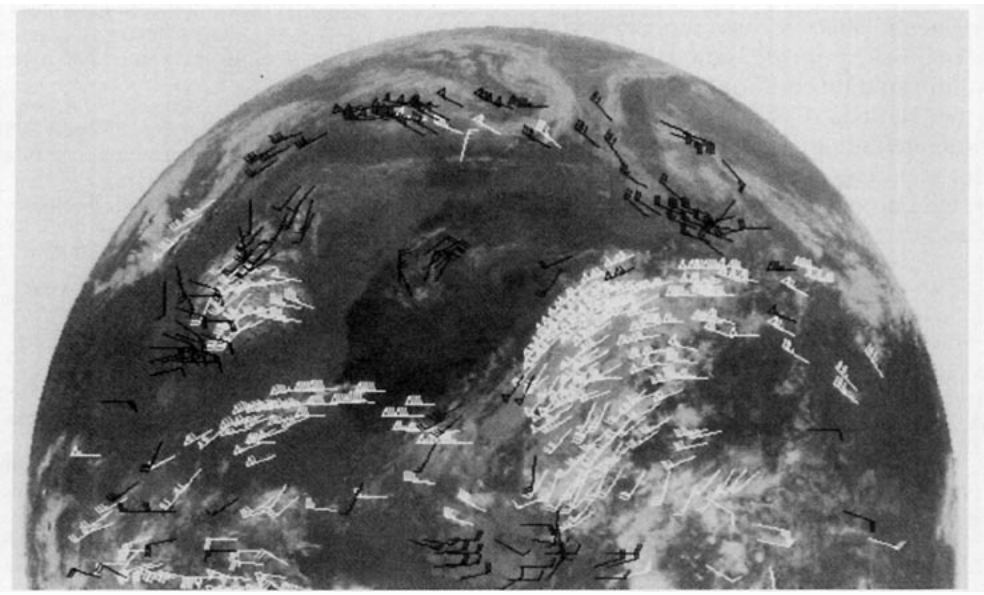

FIG. 7. ESOC operational cloud-motion vectors from *Meteosat-4* IR imagery for 1700 UTC 21 March 1992. Upper-level (100–400 hPa) vectors are indicated in white, lower-level (400–950 hPa) vectors in black.

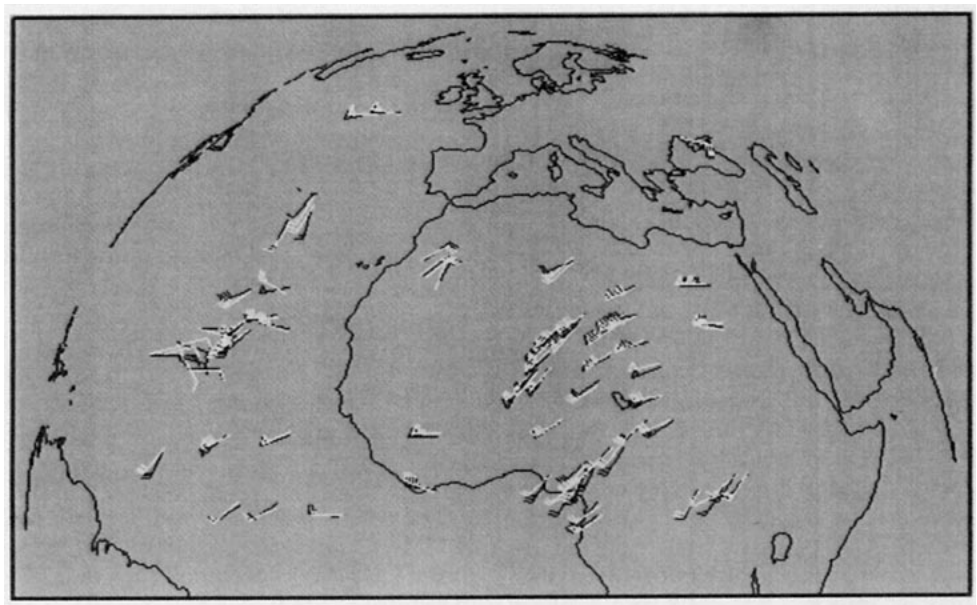

FIG. 8. Collocated cloud-motion vectors using *Meteosat-4* on 21 March 1992 from the CIMSS at 1600 UTC (white) and ESOC at 1700 UTC (black). Vectors were collocated using a tolerance of 0.5° distance.

By inference, one can conclude that the height algorithms used operationally at NESDIS (with the CO_2–IRW ratio technique) and ESOC (with their version of the H_2O–IRW intercept technique) provide similar results. The European Meteosat and the United States GOES will be maintaining the H_2O and IRW imaging capability at least for the rest of this decade. The Japanese will be launching *GMS-5* (probably in 1994), which will add an H_2O imaging capability to the existing IRW imaging capability. Thus, there is hope for international commonality in cloud-motion vector height assignment.

Acknowledgments. This work was supported in part by Contract NAG8-892 from the National Aeronautics and Space Administration and Contract 50-WCNE-8-06058 from the National Oceanic and Atmospheric Administration. Preliminary work in coding the H_2O–IRW intercept technique was done by Peter Keehn. Additionally, the European Space Agency contributed their people and expertise freely to help conduct the research.

REFERENCES

Ackerman, S. A., and W. L. Smith, 1989: IR spectral characteristics of cirrus clouds. *Proc., FIRE Science Team Meeting,* Monterey, CA, NASA, 369–373.

de Waard, J., W. P. Menzel, and J. Schmetz, 1992: Atlantic data coverage by *Meteosat-3. Bull. Amer. Meteor. Soc.,* **73,** 977–983.

EUMETSAT, 1991: Workshop on wind extraction from operational meteorological satellite data. Washington, D.C. EUMETSAT, EUM P 10, 222 pp.

ECMWF, 1992: ECMWF SATOB Data Monitoring Report, March–May 1992. European Center for Medium-Range Weather Forecasts internal paper, 16 pp.

Eyre, J. R., and W. P. Menzel, 1989: Retrieval of cloud parameters from satellite sounder data: A simulation study. *J. Appl. Meteor.,* **28,** 267–275.

Hayden, C. M., and C. S. Velden, 1991: Quality control and assimilation experiments with satellite derived wind estimates. Preprints, *Ninth Conf. on Numerical Weather Prediction,* Denver, Amer. Meteor. Soc., 19–23.

Menzel, W. P., W. L. Smith, and T. R. Stewart, 1983: Improved cloud motion wind vector and altitude assignment using VAS. *J. Climate Appl. Meteor.,* **22,** 377–384.

——, D. P. Wylie, and K. I. Strabala, 1992: Seasonal and diurnal changes in cirrus clouds as seen in four years of observations with the VAS. *J. Appl. Meteor.,* **31,** 370–385.

Merrill, R. T., 1989: Advances in the automated production of wind estimates from geostationary satellite imaging. *Fourth Conf. on Satellite Meteorology,* San Diego, Amer. Meteor. Soc., 246–249.

——, W. P. Menzel, W. Baker, J. Lynch, and E. Legg, 1991: A report on the recent demonstration of NOAA's upgraded capability to derive satellite cloud motion winds. *Bull. Amer. Meteor. Soc.,* **72,** 372–376.

Rossow, W. B., F. Mosher, E. Kinsella, A. Arking, M. DeBois, E. Harrison, P. Minnis, E. Ruprecht, G. Seze, C. Simmer, and E. Smith, 1985: ISCCP cloud algorithm intercomparison. *J. Climate Appl. Meteor.,* **24,** 877–903.

Schmetz, J., K. Holmlund, J. Hoffman, B. Strauss, B. Mason, V. Gaertner, A. Koch, and L. van de Berg, 1993: Operational cloud motion winds from Meteosat infrared images. *J. Appl. Meteor.,* **32,** 1206–1225.

Space Science and Engineering Center, 1985: Cloud drift winds. McIDAS Applications Guide, SSEC Report, 331 pp. [Available from the University of Wisconsin–Madison, Madison, WI 53706.]

Suomi, V. E., R. Fox, S. S. Limaye, and W. L. Smith, 1983: McIDAS III: A modern interactive data access and analysis system. *J. Climate Appl. Meteor.,* **22,** 714–724.

Szejwach, G., 1982: Determination of semi-transparent cirrus cloud temperature from infrared radiances: Application to Meteosat. *J. Appl. Meteor.,* **21,** 384–393.

Tomassini, C., 1981: Objective analysis of cloud fields. *Proc. Satellite Meteorology of the Mediterranean,* ESA (European Space Agency) SP-159, 73–78.

Wylie, D. P., and W. P. Menzel, 1989: Two years of cloud cover statistics using VAS. *J. Climate,* **2,** 380–392.